Silicone Embedded FBGs for Force Sensing

P. Di Palma, E. De Vita, A. Iadicicco, and S. Campopiano(✉)

Department of Engineering, University of Naples "Parthenope", Naples, Italy
stefania.campopiano@uniparthenope.it

Abstract. Force sensing is spreading in many fields, spanning from biomedicine to robotics. Commercial and traditional solutions include strain gauges and micro-electro-mechanical systems, that however exhibit drawbacks related to their electrical nature, fragility, and not flexible structure. Therefore, in this work, a flexible force sensor based on the fiber Bragg grating (FBG) embedded in a silicone patch is proposed and characterized. Silicone embedding represents the solution for handling a soft, stretchable, safe, and skin-mountable force sensor suitable for human interactions. Force tests are reported and demonstrate the silicone patch capability to make the FBG sensitive to force variations with good linearity and a force sensitivity of 17.6 pm/N. Moreover, the performances of the developed patch in terms of temperature and strain are compared with respect to the more traditional FBGs embedded in 3D printed PLA patch. The comparison reveals the strong influence, and complementarity, of the patch materials employed for the embedding on the sensing potentialities of the final devices.

Keywords: Fiber Bragg grating · Fiber optic sensor · Force sensor · Silicone embedding

1 Introduction

Fiber Bragg gratings (FBGs) represent a sensing solution able to provide many advantageous features, from wavelength division multiplexing to immunity to electromagnetic interferences, non-toxicity, biocompatibility, and electrical safety. A peculiar aspect is given by their small size, which makes them suitable for easy installation and embedding procedures into a variety of materials and structures. FBG-embedding strategies can be implemented for several reasons: i) for sensing purposes, i.e., to make FBGs responsive to specific parameters, such as pressure [1], curvature [2], and 3D shape [3]; ii) to package the sensing element aiming to protect the fragile regions of the optical fiber, [4]; iii) to enable smart structures, by integrating them with FBGs for design validation and damage detection [5], or by sensorizing robotic fingers and skin [6].

One of the FBG embedding techniques is represented by the embedding during manufacturing, with which the optical fiber is directly integrated into the composite laminate during its manufacturing. For this reason, 3D printing based on the fused deposition method (FDM), which lies in a continuous stacking of physical layers, matches well with FBG embedding needs. By implementing this strategy, FBGs can be easily

G. Cocorullo et al. (Eds.): SIE 2022, LNEE 1005, pp. 160–165, 2023.
https://doi.org/10.1007/978-3-031-26066-7_25

embedded in patches made with resin and plastic materials like acrylonitrile butadiene styrene (ABS) and polylactic acid (PLA) [7, 8].

However, due to the arising interest in biomedical purposes, robotics applications and, more specifically, soft robots in domestic and healthcare environments, the demand for flexible, skin-mountable, and wearable electronic devices is increasing toward safer sensing systems able to smoothly interact with the human body as well as to handle fragile objects. Therefore, in this work, silicone matrix has been investigated and used as substrate material to realize a flexible FBG-based patch. Thanks to the embedding inside the silicone matrix, the FBG not only can be protected in a soft material able to adapt its shape to the environment but has proved also to be sensitive to the variations of transversal forces acting. Such sensor overcomes the typical disadvantages of traditional electrical force sensors, being flexible, stretchable, and with a moldable shape [9].

The aim of this work is to quantitatively describe the performances of the developed silicone FBG-based patch and to compare it with FBGs embedded in more traditional materials, such as 3D printed PLA patches. Results show that silicone embedding insulates the FBG from strain variations while allowing measurements of force variations acting on the patch.

2 Materials and Methods

The proposed sensor consists in a silicone flexible patch embedding an FBG having a length of 10 mm and positioned at the center of the patch.

An FBG is a periodic perturbation of the refractive index in the optical fiber core witch, in presence of a broadband light, reflects a very narrow band centered around the Bragg wavelength (i.e., λ_B), specific for that FBG [10]. Since both thermal and strain variations induce a λ_B shift, FBGs are sensitive to both these parameters by means of a thermal and strain sensitivity, which typical values are 10 pm/°C and 1.2 pm/με, respectively, for a bare FBG.

In a preliminary phase, the process to realize the sensing device involved the 3D printing technology to realize the mold in which the silicone patch has been obtained afterward. In particular, Renkforce RF500 3D printer and the FDM have been employed for manufacturing the mold in PLA filament, produced by Renkforce. Once printed the mold, the fabrication of the FBG embedded in the silicone matrix was performed in six stages, as described in Fig. 1.

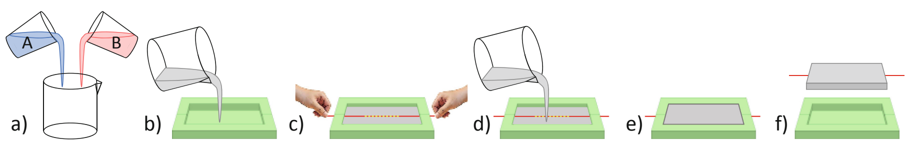

Fig. 1. Fabrication steps of the silicone patch embedding the FBG sensor: a) mixing of the two silicone components; b) pouring of half of the mixture in the mold; c) FBG positioning; d) pouring of the remaining half of the silicone; e) curing; f) patch extraction from the mold.

The process started with the preparation of the silicone matrix, i.e., Dragon Skin™ (DS) 10 Medium, by mixing its two components in equal amounts (Fig. 1a). Then, half of the mixture was poured in the mold (Fig. 1b), in such a way that the optical fiber containing a bare FBG could be positioned in the center (Fig. 1c); subsequently, the remaining mixture was poured over (Fig. 1d). Finally, after a curing time of five hours (Fig. 1e), the device was removed from the mold, obtaining a silicone patch, 2.5 mm thick, ready to be used (Fig. 1f).

3 Results and Discussion

In this section, the results of the thermal and strain characterizations of the silicone patch are reported and compared with the ones obtained by a previously developed 3D printed PLA patch, 1.8 mm thick embedding an FBG having a length of 10 mm (as for the FBG embedded in the silicone patch) [11]. Moreover, the force characterization is reported, demonstrating the silicone embedding capability to make FBGs sensitive to force variations acting on the patch.

The results related to the thermal characterization are reported in Fig. 2. In particular, Fig. 2a shows the schematic of the experimental setup used during the thermal tests, whereas Fig. 2b reports the profiles of Bragg wavelength variation $\Delta\lambda$ as function of temperature T recorded by the silicone (in red) and the PLA (in blue) patches, each one compared with the profile recorded by the bare FBG (in black). Beyond optical interrogator, FBG patches, and PC to process sensor data, the experimental setup includes a thermal chamber to perform the tests from 5 °C to 40 °C.

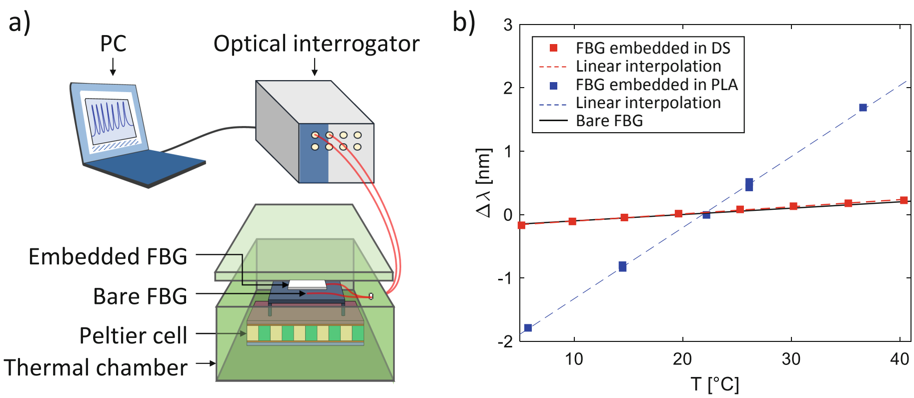

Fig. 2. Thermal characterization: sketch of the implemented experimental setup (a) trends of $\Delta\lambda$ as function of T recorded by the FBG embedded in the silicone patch, in red, and the one embedded in the PLA patch, in blue (b). Black profile corresponds to the bare FBG.

Trends reported in Fig. 2b show a linear behavior in temperature for both patches but with very different thermal sensitivities, i.e., 11.3 pm/°C for the silicone patch and 112.3 pm/°C for the PLA patch. Such results reveal that silicon matrix causes only a slight increase of the thermal sensitivity of the bare FBG, whereas the PLA is responsible for a noticeable thermal sensitivity increase of more than ten time, due to the higher thermal expansion coefficient of the PLA, which is around 80 $\mu m \cdot m^{-1} \cdot °C^{-1}$ against

6 μm·m^{-1}·°C^{-1} of the silica. Actually, the silicone thermal expansion coefficient is about four times higher than PLA one, but the measured sensitivity value is close to the bare FBG sensitivity due to the high elasticity of the silicone.

Concerning the tests for the strain characterization, the experimental setup shown in in Fig. 3a was used: to induce a strain variation in the embedded FBGs, both silicone and PLA patches were bonded on a beam together with a bare FBG as reference, and the beam was bent by means of loads ranging from 2 kg to 6 kg.

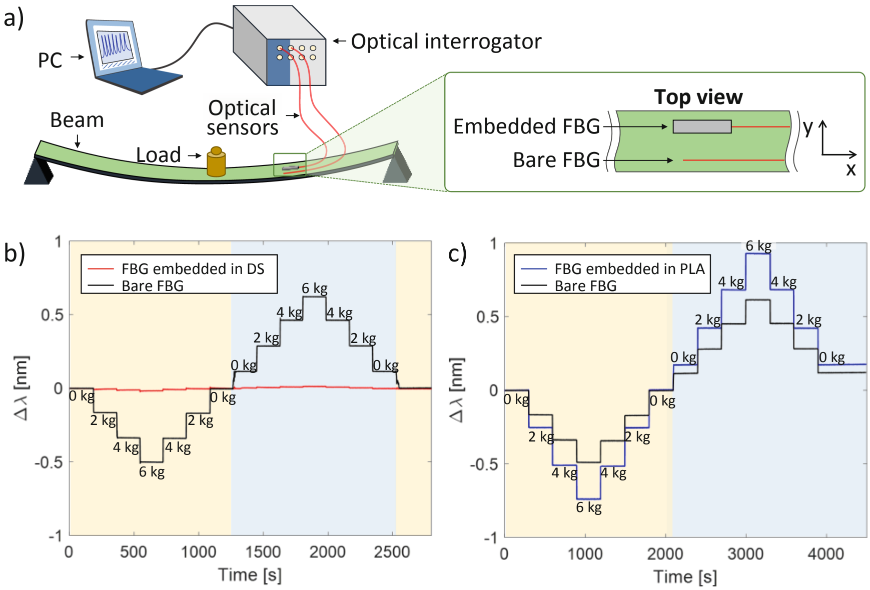

Fig. 3. Strain characterization: sketch of the implemented experimental setup (a) trends of Δλ as function of time recorded by the FBG embedded in the silicone patch, in red (b) and the one embedded in the PLA patch, in blue (c). Profiles steps correspond to increasing and decreasing loads, whereas the profile recorded by the bare FBG is reported in black. The yellow and blue squares in (b) and (c) correspond to the test performed with the sensors on the upper and bottom sides of the beam, respectively.

Figure 3b and Fig. 3c report the Δλ profiles as function of time recorded by the silicone (in red) and PLA (in blue) patches, respectively, whereas the profile recorded by the bare FBG is shown in black. These results demonstrate that, the PLA patch preserves the same strain sensitivity of the FBG bare (i.e., 1.2 pm/με), since the slight increase of the sensitivity value is not due to the plastic material, but rather to the higher distance of the embedded FBG from the neutral axis with respect to the bare one. On the contrary, silicone embedding does not transmit the strain solicitation from the external surface of the patch to the internal FBG, resulting in the insulation of the sensor from strain variations. Indeed, the strain sensitivity of the silicone patch is $3.1 \cdot 10^{-2}$ pm/με.

The measured thermal and strain sensitivities for the bare FBG and the FBGs embedded in silicone and PLA patches are summarized in Table 1.

Table 1. Silicone embedded, PLA embedded, and bare FBGs: comparison among their temperature and strain sensitivities.

	Temperature sensitivity [pm/°C]	Strain sensitivity [pm/$\mu\varepsilon$]
FBG in silicone patch	11.3	$3.1 \cdot 10^{-2}$
FBG in PLA patch	112.3	1.2
Bare FBG	10.0	1.2

Finally, force characterization proves the capability of the developed silicone patch to measure force variations exerted on the patch itself. The working principle is based on the expansion of the silicone matrix in the plane orthogonal with respect to the compression direction when a distributed load is applied to the upper surface of the patch, as shown in Fig. 4a.

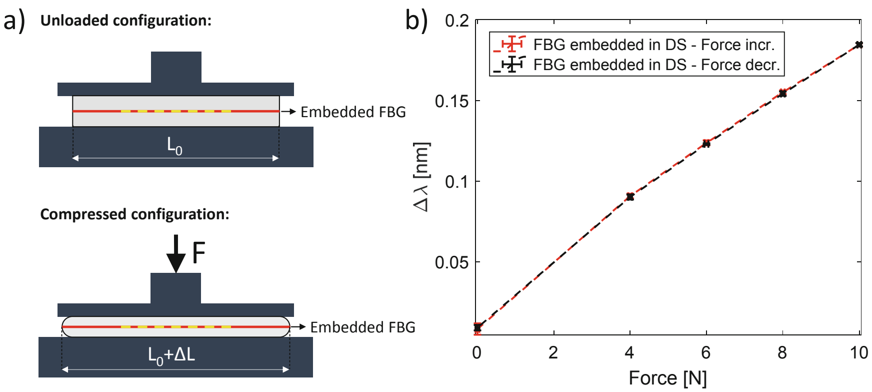

Fig. 4. Force characterization: sketch of the implemented experimental setup (a) and trend of $\Delta\lambda$ recorded by the FBG embedded during force increasing (in red) and decreasing (in black).

The force characterization result is reported in Fig. 4b. A force sensitivity of 17.6 pm/N was found, demonstrating good linearity, repeatability, and absence of hysteresis in the investigated range, i.e., from 0 to 10 N.

4 Conclusions

In conclusion, this work demonstrates the effectiveness of silicone embedded FBGs for force sensing, realizable by means of a simple fabrication process and a low-cost setup. Several novelties are worth to be highlighted in comparison to literature, such as the device flexibility due to the silicone material, allowing to obtain a sensing device easily adaptable to irregular supports. Moreover, the sensor is not affected by tensile strain, differently from the common embedded sensors reported in literature.

It is worth noting that the developed silicone patch shows complementary performances with respect to the previously developed 3D printed patch in PLA, as demonstrated by the experimental results reported in Fig. 2 and Fig. 3. Indeed, while PLA patch increases the temperature sensitivity of the FBG, keeping constant the strain sensitivity, the silicone patch desensitizes the FBG with respect to strain variations, keeping almost constant its thermal sensitivity and making the FBG sensitive to the force variations acting on the patch. These results lead to a flexible FBG-based patch with a strain sensitivity independent from the material where the patch is fixed and facilitating the temperature compensation operation.

References

1. Hong, C., Zhang, Y., Borana, L.: Design, fabrication and testing of a 3D printed FBG pressure sensor. IEEE Access. **7**, 38577–38583 (2019)
2. Di Palma, P., Iadicicco, A., Campopiano, S.: Curvature sensor based on FBGs embedded in 3D printed patches. IEEE Sens. J. **21**(16), 17868–17874 (2021)
3. Di Palma, P., De Vita, E., Iadicicco, A., Campopiano, S.: 3D shape sensing with FBG-based patch: from the idea to the device. IEEE Sens. J. **22**(2), 1338–1345 (2022)
4. Manzo, N. R., Callado, G.T., Cordeiro, C.M, Vieira Jr., L.C. M.: Embedding optical fiber Bragg grating (FBG) sensors in 3D printed casings. Opt. Fiber Technol. **53**, 102015 (2019)
5. Beukema, R.P.: Embedding technologies of FBG sensors in composites: technologies, applications and practical use. In: 6th European Workshop on Structural Health Monitoring, Dresden (EWSHM 2012), vol. 3 (2012)
6. Park, Y.-L., Chau, K., Black, R.J., Cutkosky, M.R.: Force sensing robot fingers using embedded fiber Bragg grating sensors and shape deposition manufacturing. In: Proceedings 2007 IEEE International Conference on Robotics and Automation, pp. 1510–1516. IEEE (2007)
7. Di Palma, P., Iadicicco, A., Campopiano, S.: FBGs in 3D printed objects monitoring. In: 2021 IEEE International Workshop on Metrology for Industry 4.0 IoT, pp. 182–186. IEEE (2021)
8. Lin, Y.K., Hsieh, T.S., Tsai, L., Wang, S.H., Chiang, C.C.: Using three-dimensional printing technology to produce a novel optical fiber Bragg grating pressure sensor. Sens. Mater. **28**(5), 389–394 (2016)
9. Tarchanidis, K.N., Lygouras, J.N.: Data glove with a force sensor. IEEE Trans. Instrum. Meas. **52**(3), 984–989 (2003)
10. Hill, K.O., Meltz, G.: Fiber Bragg grating technology fundamentals and overview. J. Lightwave Technol. **15**(8), 1263–1276 (1997)
11. Di Palma, P., Iadicicco, A., Campopiano, S.: Study of fiber Bragg gratings embedded in 3d-printed patches for deformation monitoring. IEEE Sens. J. **20**(22), 13379–13386 (2020)